INL/CON-22-67260-Revision-0

A review of cladding failure thresholds in RIA conditions based on transient reactor test data and the need for continued testing

October 2022

Changing the World's Energy Future

David W Kamerman, Colby B Jensen, Charles P Folsom, Nicolas E Woolstenhulme, Daniel M Wachs

Idaho National Laboratory

INL/CON-22-67260-Revision-0

A review of cladding failure thresholds in RIA conditions based on transient reactor test data and the need for continued testing

David W Kamerman, Colby B Jensen, Charles P Folsom, Nicolas E Woolstenhulme, Daniel M Wachs

October 2022

Idaho National Laboratory
Idaho Falls, Idaho 83415

http://www.inl.gov

Prepared for the
U.S. Department of Energy
Under DOE Idaho Operations Office
Contract DE-AC07-05ID14517

A review of cladding failure thresholds in RIA conditions based on transient reactor test data and the need for continued testing

David Kamerman, Colby Jensen, Charles Folsom, Nicolas Woolstenhulme, Daniel Wachs

**Idaho National Laboratory, 1955 North Fremont Avenue, Idaho Falls, ID, United States*
david.kamerman@inl.gov

[leave space for DOI, which will be inserted by ANS]

INTRODUCTION

Transient reactor experiments on light water reactor (LWR) fuel pins have been conducted since the beginning of the nuclear era to help determine core coolability and cladding failure thresholds. During one such test in November of 1993, at the CABRI transient test reactor, it was discovered that cladding failures could occur independent of a departure from nucleate boiling (pre-DNB) event. The test involved a fuel rod at high burnup with corroded, and subsequently hydrided, Zircaloy-4 cladding. Thirteen additional tests would be performed in the CABRI reactor over the next decade on fuel rods with higher burnups [1]. The initial CARBI tests were unusual in that they tested LWR fuel pins but in flowing sodium environment. However, a larger testing program at the NSRR reactor in Japan with high burnup fuel in static water capsules would uncover a similar trend of pre-DNB ruptures in high burnup test rods at lower-than-expected peak enthalpies [2]. The generally accepted mode of failure associated with these pre-DNB ruptures is a through thickness crack initiation and propagation in hydrided cladding as the result of tensile loads generated from pellet cladding interaction [3]. The term PCMI (pellet cladding mechanical interaction) is thus often used to describe these failures. In addition to the transient reactor tests, numerous out of pile testing programs involving a variety of innovative mechanical testing techniques have been employed in an attempt to better understand the failure mechanism and quantify the failure thresholds of hydrided zirconium alloy cladding in these rapid heating and loading conditions [4][5][6][7].

While previously interim guidance had been issued, in June of 2020 the NRC officially published updated regulatory guidance to account for these pre-DNB failures in Regulatory Guide 1.236 [8]. This paper presents an independent review of the publicly available transient reactor test database on higher burnup LWR pins conducted at the CABRI and NSRR reactors. The purpose of the review is to determine how well the new regulatory limits are supported by transient test data. The review will identify if additional transient reactor tests could provide additional support for the NRC guidance or identify the need for revisions. The evaluation will consider how far the existing database can be extrapolated when considering newer zirconium alloy claddings (with and without protective coatings) with low hydrogen pickup, but which contain very high burnup (> 70 MWd/kgU) UO_2 fuel pellets. Additionally, a review of a selection of published out of pile mechanical testing methods will be conducted and the authors will suggest how out of pile mechanical tests can be used in conjunction with a limited number of transient reactor tests to develop cladding specific failure thresholds in RIA type transients.

ANALYSIS OF TRANSIENT REACTOR TESTS

A database of 82 transient reactor tests on moderate to high burnup LWR fuel pins tested in the CABRI and NSRR reactors was developed through consultation of a variety of open literature sources [1][2][9][10][11][12][13][14][15][16][17][18]. The peak fuel enthalpy, failure enthalpy (in the case of tests resulting in cladding rupture), transient pulse width, test coolant initial temperature, fuel type, fuel burnup, cladding type, cladding diameter, and thickness, observed oxide layer thickness, evaluated hydrogen content, and post transient permanent hoop strain were all documented. The value of each of these variables could not always be found for every test from primary sources however a similar effort by Beyer and Geelhood provided additional information to fill in most blanks [19]. Cladding hydrogen measurements are often calculated from oxide thickness measurements and assumed hydrogen pickup fractions for that cladding type adding some uncertainty to this parameter. Consultation of a paper by Georgenthum et al. allowed for the thickness of the hydride rim and extended hydride rim for 25 of the transient reactor tests to be included in the analysis [20]. Finally, 12 transient reactor tests at NSRR on unirradiated test rods that were artificially hydrided and filled with oversized UO_2 pellets were added to the database as it was shown that rods in this condition similarly experienced 'pre-DNB' failures [21]. Inclusion of these tests brings the size of the database up to 94 transient reactor tests.

Regulatory Guide 1.236 provides different PCMI failure limits based on initial coolant temperature and cladding type. The cut off temperature between the different limits is 500 °F (260 °C). These limits are all expressed as a peak radial average enthalpy rise. Limits start at 630 J/g (officially 150 cal/g) and begin to decrease exponentially at a specified cladding excess hydrogen threshold which differs by cladding type in addition to initial temperature. The 630 J/g enthalpy rise limit is near that of the 711 J/g (officially 170 cal/g) total enthalpy limit which corresponds to a post DNB failure mode when one accounts for the starting enthalpy of the fuel particularly in hot coolant conditions.

Cladding types are grouped into stress relieved zirconium alloys (SRA) and fully recrystallized zirconium alloys (RXA). The logic for the differentiation is the morphology of hydrides commonly seen in zirconium alloys with different heat treatments. The SRA cladding types generally form hydrides with a dominate circumferential orientation, while RXA cladding types form hydrides with a random orientation [22]. For RXA claddings the guide makes a small distinction between those with inner liners and those without. Cladding types in the developed database considered to fit into the SRA category include Zircaloy-4, low tin Zircaloy-4, stress relieved Mitsubishi Developed Alloy (MDA), stress relieved New Developed Alloy (NDA), Zirlo, and low tin Zirlo. Cladding types in the database considered to fit into the RXA category include Zircaloy-2, recrystallized MDA, and M5. 64 tests in the database consist of tests with SRA cladding while 30 consist of tests with RXA cladding.

Analysis of SRA Cladding Failure Limits

Of the 64 tests conducted with SRA cladding most of them, 47, took place at the NSRR reactor in a room temperature (cold) water capsule. Regulatory Guide 1.236 specifies a cladding excess hydrogen threshold of ~132 ppm after which the enthalpy rise limit begins to decrease exponentially to 209 J/g. Fig. 1. below shows this limit with the 47 supporting transient reactor tests. The tests with unirradiated pre-hydrided cladding are shown in lighter blue. Tests that failed are plotted against their enthalpy rise at failure while tests that did not fail are plotted against their total enthalpy rise.

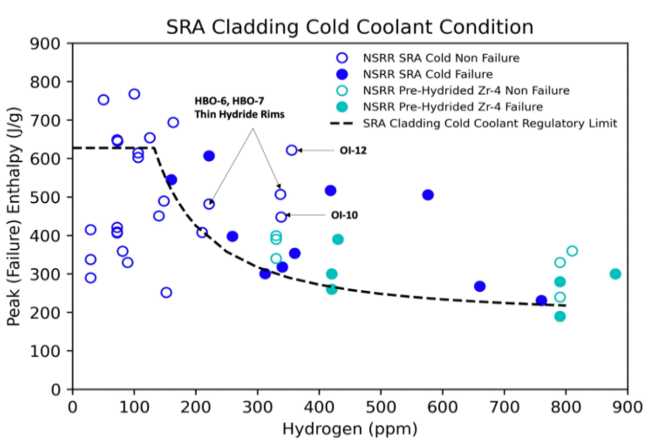

Fig. 1. Low Temperature SRA Failure Limit with supporting transient reactor tests.

The proposed failure limit above the hydrogen threshold of 132 ppm seems well supported by the database. Tests HBO-6, HBO-7, OI-10, and OI-12 are anomalous as they have higher hydrogen contents (> 300 ppm) and do not fail even at substantial enthalpy rises. Consultation of the rim thickness by Georgenthum et al. [20] provides a useful explanation for two of these tests. HBO-6 and HBO-7 have thinner hydride rims than would be expected for cladding excess hydrogen reported. The more uniform distribution of hydrides in these test samples explains their added resilience. The rim structure of OI-10 is reported as being between 50 μm and 100 μm so it is more difficult to explain why this test rod survived. No additional information on test OI-12's hydrogen structure is available but it is the only test in the database with the NDA cladding type so it is possible that an a-typical hydride structure exists in this cladding making it more resilient.

In these transient tests, instrumentation such as water pressure sensors, water column velocity detectors, and acoustic sensors are used to determine the time of failure. Enthalpy rise at failure is a calculated value that requires data from the reactor power, energy conversion factors, and heat transfer properties to be input into a thermos mechanical fuel performance code. Thus, while it is conventional to use the enthalpy rise at the time of failure values to support the development of cladding rupture limits it must be acknowledge that there is inherent uncertainty in the reported values. Using this convention, the NRC limit which primarily exists between ~300 J/g and ~200 J/g after ~300 ppm hydrogen seems to be well supported. In the pre-hydrided transients by Tomiyasu [21], tests of similarly hydrided cladding are shown to survive transients with peak enthalpy rises of 400 J/g but when subjected to a transient with a peak enthalpy rise of 550 J/g failure occurs at 260 J/g. These tests strongly imply that it would be incorrect to assume that because the test rod in the 550 J/g transient failed at 260 J/g, that such a rod would fail when subjected to a transient with a total enthalpy rise of 260 J/g. When the cladding failure cases presented in Fig. 1. are plotted with respect to their peak enthalpy rise instead of their enthalpy rise at failure much greater separation of the failure and non-failure cases is seen. This plot is shown in Fig. 2. While the observed hydrogen threshold (130 ppm - 300 ppm) does not change the failure limit would increase to around 400 J/g - 500 J/g.

Of the 17 tests that took place at elevated temperature, 5 took place in a heated version of the NSRR capsule, and the remaining 12 took place in the CABRI sodium loop. Regulatory Guide 1.236 specifies a cladding excess hydrogen threshold of ~160 ppm after which the enthalpy rise limit begins to decrease exponentially to 251 J/g. Fig 3. below shows this limit with the 17 supporting transient reactor tests. While the convention of plotting failed test pins at their enthalpy rise at the time of failure is held, annotations are added to the figure to show the peak enthalpy rise of these transients.

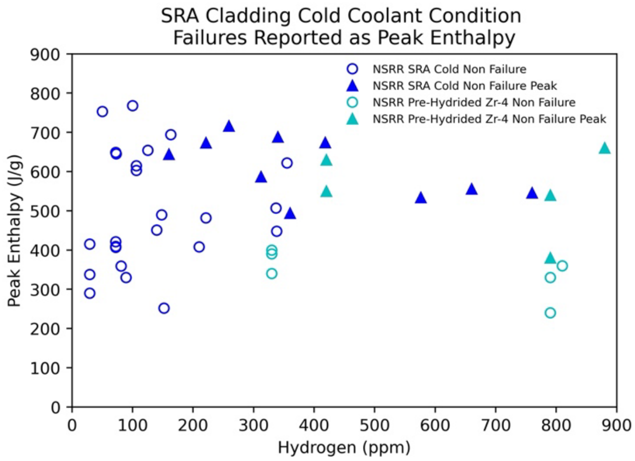

Fig. 2. Low Temperature SRA Tests with Failure Cases plotted with Respect to Peak Enthalpy.

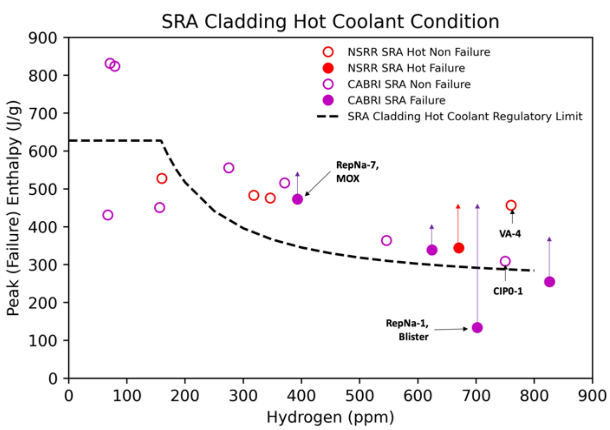

Fig. 3. High Temperature SRA Failure Limit with supporting transient reactor tests.

The contrast of the high temperature test database when compared to the low temperature test database is striking. In addition to there being dramatically fewer tests, failures are rarely seen below 500 ppm – 600 ppm cladding hydrogen with only one test pin RepNa-7, a MOX rod, failing below this threshold. The enthalpy rise limit above 500 ppm – 600 ppm appears to be supported at around 300 J/g, when considering the enthalpy rise at time of failure. However, this limit would increase to between 400 J/g – 500 J/g range if the total peak enthalpy rise were to be considered. The survival of VA-4 and CIP0-1 provide additional, albeit limited, support for the higher limit.

The high temperature dataset itself provides some initial evidence for the consideration of rate affects, as intuitively slower transients allow for more time for cladding temperature to increase at a given PCMI load and it is obvious from the data set that warmer cladding is less prone to PCMI failure at a given hydrogen level. This observation has led many to wonder if the transient pulse width is an important factor which could influence the failure limit. While all the NSRR tests take place at very narrow pulse widths between 5 ms and 10 ms, CABRI testing took place at a larger variety of pulse widths between 9 ms and 75 ms. However, there is no clear distinction in failure limit when comparing tests of similar hydrogen content, irradiated in transients with different pulse widths. There are cases of failure at pulse widths greater than 30ms (RepNa-7, RepNa-8, and RepNa-10) and many cases of survival at pulse widths less than 30ms with cladding hydrogen level being the common differentiator affecting failure or survival. Due to the efficient cooling of the Na coolant in the CABRI RepNA tests pulse width effects maybe more muted than in PWR water [23]. There are no tests of comparable hydrogen content irradiated at different pulse widths which could be used to more conclusively justify or defend a pulse width effect on the failure limit.

The NRC failure limits for SRA cladding at cold temperature are well supported by the database, although higher (less conservative) limits could be justified if peak enthalpy rise rather than enthalpy rise at the time of failure were used. Therefore, the NRC failure limits for SRA cladding at high temperature may be too conservative particularly in the range of cladding excess hydrogen levels between 160 ppm and 500 ppm. However, it is admitted that the database is particularly sparse in this region and so a conservative limit may be justified. Thus, when considering the current regulatory limits, the most useful transient tests for SRA cladding types would be tests with cladding hydrogen contents between 100 ppm and 600 ppm in a hot water capsule with peak enthalpy rises greater than 450 J/g.

Analysis of RXA Cladding Failure Limits

Of the 30 tests conducted with RXA cladding most of them (24 total) took place at the NSRR reactor in a room temperature (cold) water capsule. Regulatory Guide 1.236 specifies a cladding excess hydrogen threshold of ~62 ppm for regular cladding types and ~77 ppm for claddings with a zirconium liner after which the enthalpy rise limit begins to decrease to 138 J/g. Fig. 4 shows this limit with the 24 supporting transient reactor tests.

The proposed limit seems conservative for cladding with excess hydrogen contents between 62 ppm and 159 ppm as no failure data exists below 159 ppm hydrogen (test FK-9). Additionally most of the non failure data is at peak enthalpies below the failure limit. However, only one test with cladding hydrogen content greater that 159 ppm does not fail, test OS-2. The lack of transient reactor tests which survive even small enthalpy rises above this threshold may lead some to wonder if the proposed limit is too generous in this region. In fact, test OS-1 fails below the NRC limit. This test and OS-2, which conversely does not fail above the limit are the subject of much discussion in the community due to the use of pellet dopants in these fuel rods which may affect the test outcomes. Tests FK-10 and FK-12 were unique in that they were tested at ~80 °C to simulate warming that would occur in longer pulse widths. While the failure enthalpies for these tests is slightly higher than parallel tests FK-6 and FK-7 the difference is marginal. Thus, these tests would seem to indicate that the small amount of additional heating provided to the cladding in longer pulse width tests is insufficient to provide a notable change in the failure limit and that temperatures above 100 °C are needed for ductility recovery to become meaningful.

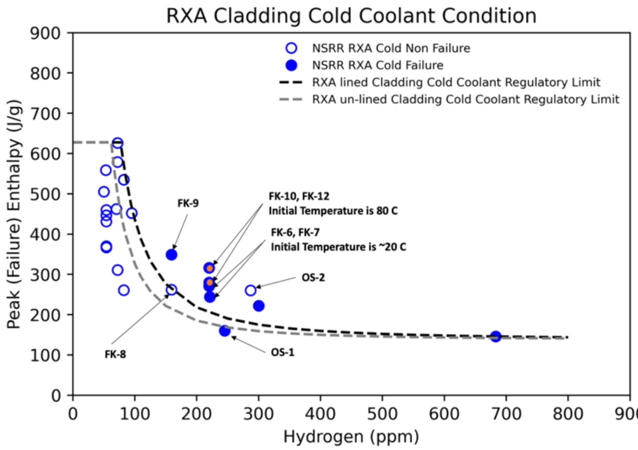

Fig. 4. Low Temperature RXA Failure Limit with supporting transient reactor tests.

Only 6 tests have taken place on RXA claddings at elevated temperatures which simulate hot zero power conditions. Four of these tests are in the NSRR hot water capsule and 2 are in the CABRI Na loop. Regulatory Guide 1.236 specifies a cladding excess hydrogen threshold of ~74 ppm for regular cladding types and ~93 ppm for claddings with a zirconium liner after which the enthalpy rise limit begins to exponentially decrease to 209 J/g. Fig. 5 shows this limit with the supporting tests. Due to the very limited number of tests at this condition it is very difficult to say that the proposed limit is either supported or not. A few tests in the NSRR hot capsule, LS2 and LS3 would seem to indicate that the limit is conservative particularly for claddings with excess hydrogen contents less than 300 ppm.

When considering the current regulatory limits, the most useful transient tests for RXA cladding types would be tests with cladding hydrogen contents between 100 ppm and 300 ppm in a hot water capsule, although more tests in the cold-water capsule would also be useful, with peak enthalpies greater than 450 J/g at a variety of pulse widths.

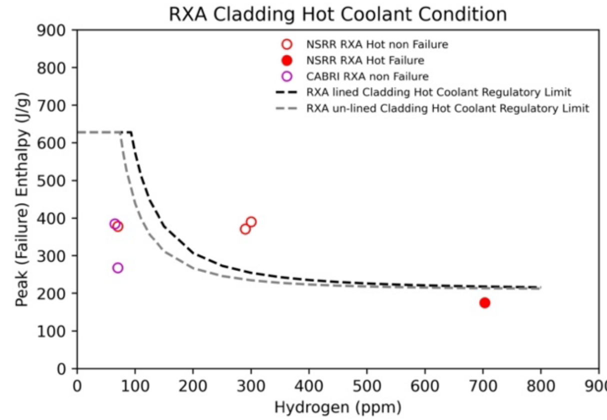

Fig. 5. High Temperature RXA Failure Limit with supporting transient reactor tests.

HIGH BURNUP UO_2 FUEL WITH LOW HYDROGEN CLADDING

Efforts are underway in the U.S. to develop accident tolerant fuel rod claddings that incorporate a coating on the zirconium alloy which dramatically reduce in-pile corrosion and hydrogen pickup [24]. Even without these novel coatings, modern alloys such as M5 and Axiom products produced by Framatome, and Westinghouse dramatically reduce hydrogen pickup from the Zr-2 and Zr-4 test rods which dominate the transient RIA database [25]. The ambitions of the U.S. industry are to use such claddings to support longer cycle lengths and higher rod average discharge burnups (75 GWd/MTU) to improve the fuel cycle economics of the current LWR operating fleet. Such a quest poses the question of whether the use of a low hydrogen PCMI failure limit is appropriate for fuel rods which contain advanced, low hydrogen claddings, but may have very high burnup (>85 GWd/MTU peak pellet) UO_2 fuel pellets. Research on the performance of high burnup fuel in Loss of Coolant Accidents (LOCA) suggest that high burnup UO2 is prone to significant fragmentation and pulverization when heated at rate of 5 °C/s with a threshold of ~700 °C [26]. The ramp rates and terminal fuel temperature in even moderate RIA transients are much more severe than those of LOCA transients, although the transients occur at high pressures, which impose a hydrostatic constraint on the fuel. Hydrostatic constraint has been shown to limit the extent of fuel pulverization in high temperature transients [27]. If fuel pellets fragment finely prior to cladding rupture during an RIA transient, they could cause a greater load on the cladding than that imposed by a (mostly) thermally expanding solid fuel pellet. Additionally, the high accumulation of Plutonium in the pellet rim region leads to non-uniform heating of the fuel pellet and volumetric expansion associated with potential melting of the fuel in the pellet rim region. While cladding strength and ductility will be improved due to the low hydrogen content, a cladding rupture with finely fragmented or molten fuel presents a greater safety concern to the reactor pressure vessel upon potential cladding breach than does solid pellets. It is therefore suitable to assess whether the current transient reactor testing database is sufficient to allow for the extrapolation of the low hydrogen limits to fuel rods with very high burnup UO_2 fuels.

Fig. 6 shows a plot of all the transient reactor tests with moderate and high burnup UO_2 tests (MOX tests removed). There are several tests with very high burnup UO_2 pellets that failed due to their cladding's high hydrogen content and so far, no evidence of finely fragmented or molten fuel coolant interactions have been reported with the test results although the transient enthalpy rises in these tests are generally below 600 J/g. Fig. 7 below shows the transient reactor test database with all the high hydrogen claddings removed and plotted against their fuel burnup. Hydrogen thresholds of 300 ppm for SRA claddings and 150 ppm for RXA claddings are used in selecting the tests to be displayed. There are very few tests above the current U.S. burnup limit of 62 GWd/MTU rod average burnup and only one test above the current U.S. industry desired limit of 75 GWd/MTU rod average burnup (also assume rod average burnup is ~6% lower than the segment values displayed).

NRC has conducted its own review of the current transient reactor database and concluded that while the current database is sufficient up to 68 GWd/MTU rod average, more testing would be required to justify the extrapolation of the current limits beyond this burnup level [28]. Conclusions from this review mirror that of the NRC review suggesting that more testing should be performed for fuels with high local burnups with peak enthalpy rises around and above the current low hydrogen limit of 627 J/g to not only assess for suitability of the failure limit but also to assess impacts of pulverized or molten fuel coolant interaction in regard to pressure boundary integrity, which may challenge the core coolability limit. This document also underscores the need for more testing at higher enthalpies for low hydrogen alloys, most of which are of the RXA type, particularly at high temperature.

While integral testing of irradiated fuel segments requires unique resources, several opportunities have been identified that will add significant value to the nuclear community. Test campaigns are recommended to focus on samples with RXA cladding types with high and very high burnup UO_2 fuel pellets. Recommended test conditions are elevated initial water temperatures (> 260 °C) and target peak enthalpy rises of 627 J/g or greater. If possible, testing should target a range of pulse widths between 5 ms and 100 ms to better understand any effects of pulse width on failure limit.

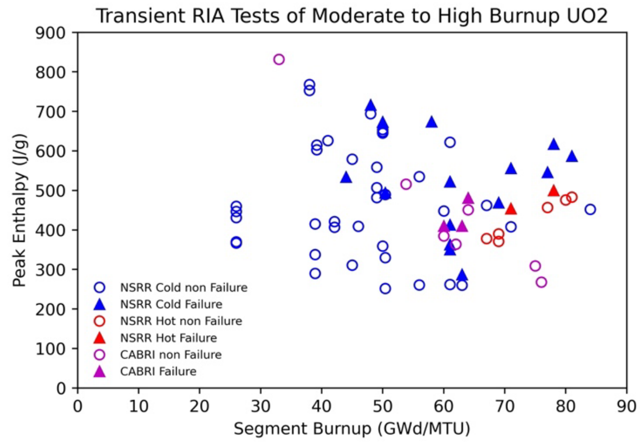

Fig. 6. Transient reactor tests with moderate to high burnup UO2 fuel plotted as function of burnup.

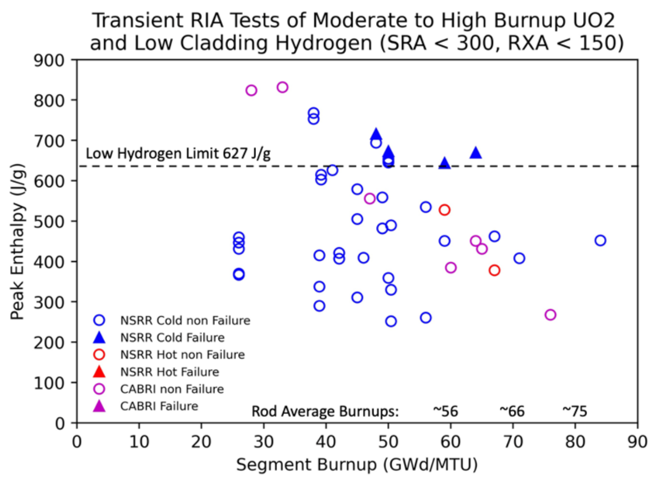

Fig. 7. Transient reactor tests with low hydrogen claddings plotted as a function of burnup.

PROPOSING CLADDING HOOP STRAIN LIMITS

If the dominate loading mechanism causing pre-DNB rupture is PCMI then the specification of cladding specific strain limits could potentially be used in place of fuel peak radial average enthalpy rise limits for assessing failure thresholds. Fig. 8. shows the residual or permanent hoop strains of transient reactor tests which did not fail, along with the maximum strain which could be imposed by a thermally expanding UO_2 fuel pellet. Tests with hoop strains below the UO_2 expansion strain likely had some amount of a pellet cladding gap or experienced a significant amount of elastic hoop strain which was recovered upon unloading. Test rods with hoop strains at or greater than the UO_2 thermal expansion strain are potentially explained by either additional loadings to the cladding such as fuel pellet gaseous expansion or transient fission gas release. Exceptionally high hoop strains may be achieved only if a boiling crisis occurs on the cladding coolant surface which is likely to have occurred in several of the NSRR tests with higher enthalpy targets. TK-1, TK-6, and TK-9 all have residual hoop strains greater than 10% and are thus not plotted in Fig. 8 and likely expanded during a boiling crisis which occurred during those tests. The RepNa-9 test was a MOX rod and saw a 7.2% residual hoop strain. Other MOX rods often see higher hoop strains than similar UO_2 rods indicating additional loading terms, other than thermal expansion, are more prevalent in MOX rods particularly when subjected to high enthalpies. Tests with UO_2 rods do not have residual hoop strains notably larger than the thermal expansion strain until ~500 J/g in the case of the hot NSRR capsule or ~600 J/g in the case of the cold NSRR capsule.

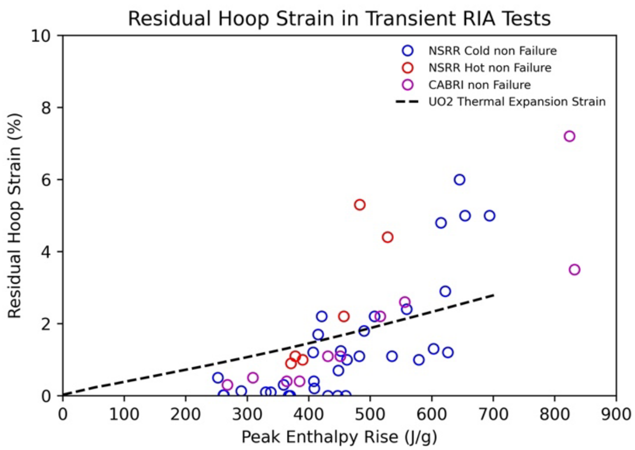

Fig. 8. Permanent hoop strain in transient reactor tests which did not fail

Analysis of Separate Effects Tests

Four separate effects test techniques are discussed below. The review of separate effects, mechanical testing presented herein is not intended to be an exhaustive review of cladding mechanical testing campaigns but rather to present an overview of available techniques and to compare the developed strain thresholds to the transient reactor test database. Three of the test campaigns discussed all involve Zr-4 (SRA) cladding with artificially hydrided cladding tubes. The modified burst test results use irradiated cladding tubes with the fuel removed.

Daum et al. [4] conducted ring tensile tests using a small gauge region designed to induce a bi-axial plane strain stress state during loading as shown in Fig. 9. These kinds of tests are referred to as plane strain tension (PST) tests. Fracture strain was measured using a series of notches in the gauge region which are examined upon failure. Tests were conducted at room temperature and at 300 °C. Several of the drawbacks of the PST tests include non-uniformity of the stress state over a very localized area of the cladding. Highly local stresses often lead to early failure.

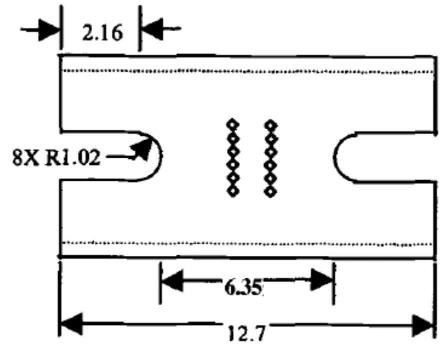

Fig. 9. Plane Strain Tension Geometry used by Daum et al. [4]

Expansion due to compression (EDC) tests seek to remedy this shortcoming by imposing the hoop strain uniformly across the entire circumference of the cladding tube. Menibus et al. [5] conducted a campaign of EDC tests with hydrided cladding. The EDC tests attempted to create a bi-axial stress state like an expanding pellet by restraining the cladding in the axial direction as shown in Fig. 10. Fracture strains reported by Menibus et al. are much larger than those reported by Daum et al. A principal drawback of the EDC test is that the expanding media begins to impose a bending moment on the cladding at relatively low hoop strains. The imposed shear stresses in the cladding allow for higher deformations than in a true bi-axial stress state as the shear stresses promote plastic flow. The fracture strains reported by Menibus et al. are likely to overestimate the hoop strain available to cladding during a transient reactor test with high principal stresses with no bending or shear terms.

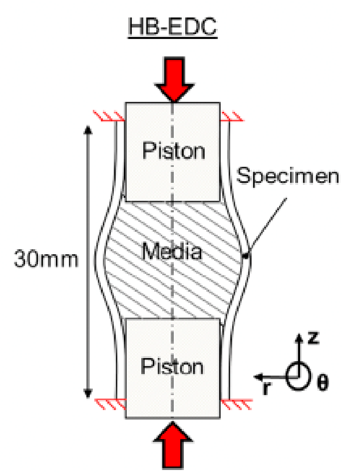

Fig. 10. Expansion due to compression tests conducted by Menibus et al. [5]

Simple burst tests do perhaps the best job of simulating a highly uniform and constrained bi-axial principal stress state in thin wall cladding tubes. Such testing has been performed by Nagase and Fuketa [6]. Nagase and Fuketa use a fluid medium to achieve very high pressurization rates like transient reactor loading rates. To achieve high temperature a nonflammable silicon oil is used. Yueh et al. [7] designed a modified burst test where the pressurizing fluid expands an Inconel 718 driver tube which is placed inside the Zircaloy-4 test sample. The modified burst test has many practical advantages on traditional burst tests when conducted in a hot cell environment as the fluid pressure boundary never ruptures and pressure fittings do not need to affix to test samples. However, in modified burst tests it is much more difficult to relate the driving pressure to sample wall stresses.

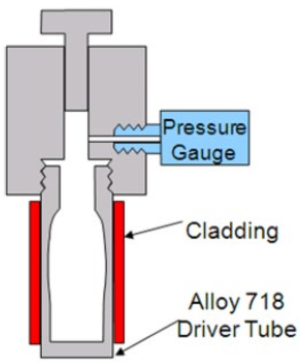

Fig. 11. Modified burst test used by Yeuh et al. [7]

Fig. 12 and Fig. 13 show the residual hoop strains of un-failed transient reactor tests with SRA cladding plotted along with the fracture strains identified in separate effects tests. The fracture hoop strain data displays notable scatter due to the varying test methods employed. Often the residual hoop strain in transient reactor RIA tests is larger than the predicted fracture strain in separate effects tests. The discrepancy is likely since the separate effects tests take place in isothermal conditions while the transient reactors tests result in a rapid heating in addition to a rapid loading of the cladding. Additionally, the condition of the hydrides in the pre-hydrided test samples used in separate effects tests do not always mirror those present from typically irradiated fuel rods (e.g. hydride blisters in the Menibus [5] study vs more common hydride rims). In very few of the separate effects tests are strain measurements performed in-situ and only in traditional burst tests is it possible to quantify the cladding wall stresses during the tests.

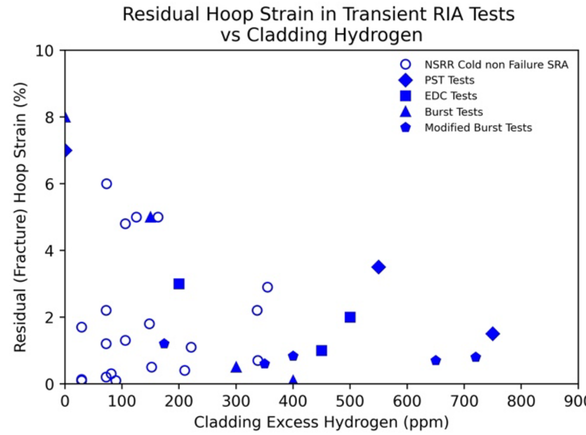

Fig. 12. Residual hoop strain in cold transient reactor tests with fracture strains developed from separate effects test data

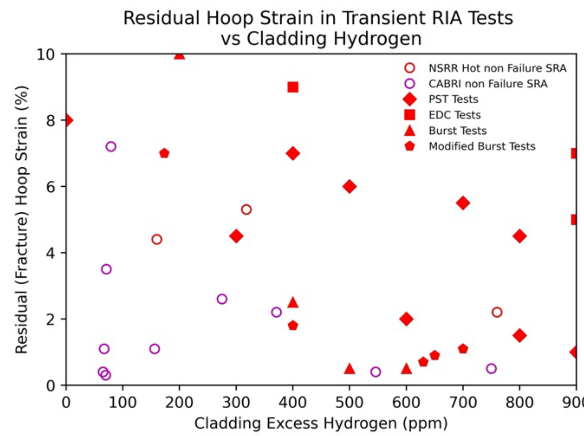

Fig. 13. Residual hoop strain in hot transient reactor tests with fracture strains developed from separate effects test data

Design Requirements for an Ideal Separate Effects Test

Brittle fractures are the result of stored energy in the material matrix while ductile fractures are the result of void formation and coalescence when available ductility is exhausted. In an ideal separate effect test, one would not only aim to simulate the loading conditions but also quantify both the amount of elastic strain energy stored in the cladding and the amount of equivalent plastic strain the sample experienced prior to rupture (brittle failure) or necking (ductile failure). While these values can be computed for the tests in question given an appropriate stress/strain constitutive relationship, available stress/strain correlations are often built upon uni-axial test data and many times do not account for the effect of hydrogen present in the cladding. Simple burst tests offer a straightforward way of creating a quantifiable bi-axial stress state in semi-thin-walled cladding tubes. Both the axial and hoop stress can be determined from knowledge of the internal pressure value. If the burst test is incorporated into a mechanical load frame, then an independent axial constraint term can be added which is necessary when isotropic yielding cannot be assumed as is often the case in textured zirconium alloys. Both the axial and hoop strain should be measured in-situ so that stress strain correlations can be developed. The use of strain gauges, extensometers, or digital image correlation equipment can be used for this application given a suitable temperature for the measurement devices. Fig. 14 shows a schematic of the described test stand where a constant hoop strain rate test can be conducted using a computer controller to adjust the pressure in the test sample using a PID feedback loop. Fig. 15 shows sample test data from a commissioning test of this setup using a fresh Zircaloy-4 rod at room temperature.

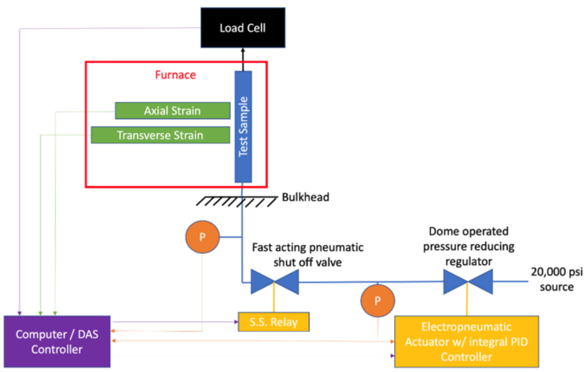

Fig. 14. Schematic of Burst Test Stand

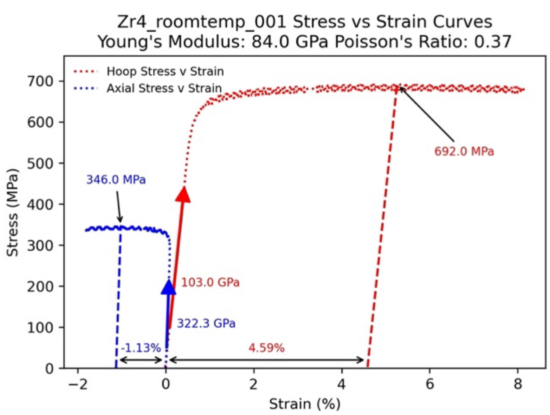

Fig. 15. Multi-axial Stress/Strain Data from Burst Test Commissioning at Room Temperature

CONCLUSIONS

This review concludes that the regulatory guidance for cladding failure due to PCMI during transient RIA analysis is well supported for SRA and RXA cladding types at low temperature. For SRA cladding types at high temperature the limits are supported at high cladding hydrogen levels but may be conservative at moderate and low hydrogen levels. Data for RXA claddings at high temperature is insufficient to make a conclusion. The need for more in-pile transient RIA testing of irradiated fuel rods with RXA claddings with low to moderate excess hydrogen levels and high to very high burnup UO_2 pellets in a hot water capsule is underscored by this review.

For cladding hoop strain evaluation, several out-of-pile separate effects testing techniques were evaluated in relation to existing data. The goal of such testing should be to develop cladding-specific failure limits. While simply determining a hoop strain limit would be convenient, it may be more appropriate to express cladding failure limits in terms of maximum equivalent plastic strain for ductile failures or an elastic strain energy density limit for brittle failure. Separate effects tests should, if possible, make use of irradiated cladding materials. As a lesser alternative, artificial hydride structures can be used, with careful consideration in their creation to ensure hydride structures are prototypic of those that form in the cladding type in question. The controlled loading conditions of the burst test method, where cladding hoop and axial strain are measured concurrently, are argued to be the most effective for analyzing material behavior and aiding in determining a relevant failure limit. Data of this kind should serve in interpreting the limited number of in-pile transient reactor RIA tests that can be performed.

ACKNOWLEDGMENTS

This work was supported through the Department of Energy Advanced Fuels Campaign under DOE Idaho Operations Office Contract DE-AC07-05ID14517. Accordingly, the U.S. Government retains and the publisher, by accepting the article for publication, acknowledges that the U.S. Government retains a nonexclusive, paid-up, irrevocable, world-wide license to publish or reproduce the published form of this manuscript, or allow others to do so, for U.S. Government purposes.

REFERENCES

1. Papin J., Cazalis B., Frizonnet M., Desquines J., Lemoine F., Geogenthum V., Lamare F., Petit M., “Summary and interpretation of the CABRI REP-Na program,” *Nuclear Technology*, Vol 157, No 3 (2017).
2. Udagawa, Yutaka., Sugiyama, Tomoyuki., Amaya, Masaki., "Thresholds for failure of high-burnup LWR fuels by Pellet Cladding mechanical interaction under reactivity-initiated accident conditions" *Journal of Nuclear Science and Technology* Vol 56:12 (2019)
3. Fuketa T. “Transient Response of LWR Fuels (RIA)” *Comprehensive Nuclear Materials* 2.22 (2012)
4. Daum R.S., Majumdar S., Bates D.W., Motta A.T., Koss D.A., Billone M.C. “On the Embrittlement of Zircaloy-4 Under RIA Relevant Conditions” *Zirconium in the Nuclear Industry: Thirteenth International Symposium, ASTM STP 1423* (2002) pp 702-719
5. Hellouin de Menibus A., Auzoux Q., Monagabure P., Macdonald V., Le Jolu T., Besson J., Crepin J., “Fracture

of Zircaloy-4 cladding tubes with or without hydride blisters in uniaxial to plane strain conditions with standard and optimized expansion due to compression tests” *Materials Science and Engineering* Vol 604 (2014)

6. Nagase F., Toyoshi F., “Investigation of Hydride Rim Effect on Failure of Zircaloy-4 Cladding with Tube Burst Test” Journal of Nuclear Science and Technology Vol 42 (2005)
7. Yueh K., Karlsson J., Stjarnsater J., Schirire D., Ledergerber G., Munoz-reja C., Hallstadius L., “Fuel cladding behavior under rapid loading conditions” *Journal of Nuclear Materials* Vol. 469 (2016)
8. Clifford, P. *Pressurized-Water Reactor Control Rod Ejection and Boiling Water Reactor Control Rod Drop Accidents* U.S. Nuclear Regulatory Commission Regulatory Guide RG 1.236, June 2020
9. Romano A., Wallin H., Zimmermann M.A., Chawla R., "Modelling the CABRI high-burnup RIA test CIP0-1 using an extended version of the FALCON code" *Nuclear Engineering and Design* 236 (2006) pp 284-294
10. Fuketa, Toyoshi., Mori, Yukihide., Sasajima., Hido., Ishijima Kiyomi., Fujishiro, Toshio., "Behavior of High Burnup PWR Fuel Under a Simulated RIA Condition in the NSRR" *Specialist Meeting on Transient Behavior of High Burnup Fuel*; Cadarache France (1995)
11. Fuketa, Toyoshi., Sasajima Hideo., Sugiyama, Tomoyuki., "Behavior of High Burnup PWR Fules with Low-Tin Zircaloy-4 Cladding under Reactivity-Initiated Accident Conditions" *Nuclear Technology* Vol 133:1 (2001)
12. Fuketa, Toyoshi., Sugiyama, Tomoyuki., Nagase, Fumihisa., "Behavior of 60 to 78 MWd/kgU PWR Fuels under Reactivity-Initiated Accident Conditions " *Journal of Nuclear Science and Technology* Vol 43:9 (2006)
13. Sugiyama, Tomoyuki., Umeda, Mika., Sasajima, Hideo., Suzuki, Motoe., Fuketa, Toyoshi., "Effect of Initial Coolant Temperature on Mechanical Fuel Failure under Reactivity-Iniated Accident Conditions" *Proceedings of Topfuel 2009*; Paris France (2009)
14. Udagawa, Yutaka., Sugiyama, Tomoyuki., Amaya, Masaki., "Thresholds for failure of high-burnup LWR fuels by Pellet Cladding mechnical interaction under reactivity-initiated accident conditions" Journal of Nuclear Science and Technology Vol 56:12 (2019)
15. Nakamura, T., Kusagaya K., Fuketa T., Uetsuka H., "High Burnup BWR Fuel Behavior Under Simulated Reactivity Initiated Accident Conditions" *Nuclear Technology* 138 (2002) pp 246-259
16. Nakamura, T., Fuketa T., Sugiyama T., Sasajima H., "Failure Thresholds of High Burnup BWR Fuel Rods under RIA Conditions" *Journal of Nuclear Science and Technology* 41 (2004) pp 37-43
17. Nakamura, T., Yoshinaga M., Sobajima M., Ishijima K., Fujishiro T., "Boiling Water Reactor Fuel Behavior at Burnup of 26 GWd/tonne U Under Reactivity-Initiated Accident Conditions" *Nuclear Technology* 108 (1994) PP 45-60
18. Mihara T., Kakiuchi K., Taniguchi Y., Udagawa Y., “Follow-up Experimental Study on the Causes of the Low-Enthalpy Failure Observed in the Reactivity-Initiated Accident-Simulated Test on LWR Additive Fuels” *Proceedings TopFuel 2021*: Santander Spain (2021)
19. Beyer C.E., Geelhood K.J., *Pellet Cladding Mechanical Interaction Failure Threshold for Reactivity Initiated Accidents for Pressurized Water Reactors and Boiling Water Reactors* PNNL-22549 (2013)
20. Georgenthum, V., Sugiyama T., Udagawa Y., Fuketa T., Desquines J., "Fracture Mechanics Approach for Failure Mode Analysis on CABRI and NSRR RIA Tests" *Proceedings 2008 Water Reactor Fuel Performance Meeting*; Seoul Korea (2008)
21. Tomiyasu K., Sugiyama T., Fuketa T., "Influence of Cladding-Peripheral Hydride on Mechanical Fuel Failure under Reactivity-Initiated Accident Conditions” *Journal of Nuclear Science and Technology* Vol. 44 No. 5 (2007) pp. 733-742
22. Clifford P. *Memorandum to Timothy J. McGinty: Technical and Reulatory Basis for the Reactivity-Initiated Accident Acceptance Criteria and Guidance, Revision 1*., ML 14188C423 (2015)
23. Ozer et al. “Assessment of Reactivity Transient Experiments with High Burnup Fuel,” *proc 23rd water reactor safety information meeting* Oct 23-25, 1995, in NUREG/CP-0149 Vol 1
24. *Roadmap: Development of Light Water Reactor Fuels with Enhanced Accident Tolerance,* Idaho National Laboratory unpublished report 2012, INL/EXT-12-25305.
25. Daun Z., Yang H., Satoh Y., Murakami K., Kano S., Zhao Z., Shen J., Abe H., “Current status of materials development of nuclear fuel cladding tubes for light water reactors” *Nuclear Engineering and Design* Vol 316 (2017) pp 131-150
26. Bales M., Chung A., Corson J., Kyriazidis L., *Interpretation of Research on Fuel Fragmentation, Relocation, and Dispersal at High Burnup* RIL 2021-13 (2021)
27. Turnbull J.A., Yagnik S.K., Hirai M., Staicu D.M., Walker C.T., “An assessment of the Fuel Pulverization Threshold During LOCA-Type Temperature Transients” *Nuclear Science and Engineering* 179:4 (2015) pp 477-485
28. Clifford P. *Memorandum to Joseph E Donoghue: Regulatory Guide 1.236 Fuel Rod Burnup Range of Applicability* ML20090A308 (2020)